Case Studies in Thermal Engineering 69 (2025) 105947

Contents lists available at ScienceDirect

Case Studies in Thermal Engineering

journal homepage: www.elsevier.com/locate/csite

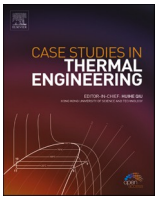

Numerical analysis of entropy generation and heat transfer of ternary nanofluids under a periodic magnetic field in a square enclosure

Seyyed Masoud Seyyedi [a,b,*], Mehdi Hashemi-Tilehnoee [c], Elena Palomo del Barrio [c,d], Humaira Yasmin [e,f], Mohsen Sharifpur [g,h,i,**]

[a] Department of Mechanical Engineering, Aliabad Katoul Branch, Islamic Azad University, Aliabad Katoul, Iran
[b] Energy Research Center, Aliabad Katoul Branch, Islamic Azad University, Aliabad Katoul, Iran
[c] Centre for Cooperative Research on Alternative Energies (CIC EnergiGUNE), Basque Research and Technology Alliance (BRTA), Alava Technology Park, Albert Einstein 48, 01510, Vitoria-Gasteiz, Spain
[d] IKERBASQUE Basque Foundation for Science, Plaza Euskadi 5, 48009, Bilbao, Spain
[e] Department of Basic Sciences, General Administration of Preparatory Year, King Faisal University, P.O. Box 400, Al Ahsa 31982, Saudi Arabia
[f] Department of Mathematics and Statistics, College of Science, King Faisal University, P.O. Box 400, Al Ahsa, 31982, Saudi Arabia
[g] Department of Mechanical and Aeronautical Engineering, University of Pretoria, Pretoria, 0002, South Africa
[h] School of Mechanical, Industrial and Aeronautical Engineering, University of the Witwatersrand, Private Bag 3, Wits, 2050, South Africa
[i] Department of Medical Research, China Medical University Hospital, China Medical University, Taichung, Taiwan

A R T I C L E I N F O

Keywords:
Natural convection
Coefficient of performance
Entropy generation
CVFEM
Ternary nanofluid
Periodic magnetic field

A B S T R A C T

Ternary nanofluids are a new class of working fluids that exhibit greater heat transfer and stability properties than single nanofluids. The main goal of the present work is to investigate the effects of a periodic magnetic field on natural convection and entropy generation in a square enclosure filled with a ternary nanofluid (Cu-Al_2O_3-Fe_3O_4-water). To achieve the stated purpose, the equations that govern energy, mass, and momentum conservation are first constructed and then transformed into non-dimensional forms using the notion of parameters with no dimension. Secondly, they are numerically solved by the Control Volume Finite Element Method (CVFEM), and the entropy generation number is calculated. The effects of active parameters such as the Rayleigh number, the volume fraction of nanoparticles, the Hartmann number, and the period number, are investigated concerning the average Nusselt number and the entropy generation number. The results were compared with those of the literature and good agreement was observed. The results discovered that there is a maximum value for Nu_{ave} and a minimum value for N_{gen} when the period number is changed for a given Hartmann number. Nu_{ave} and N_{gen} have the highest and lowest values at $\lambda = 0.7$ and $\lambda = 0.6$, respectively. Also, the value of N_{gen} decreases 16.7 % at $Ha = 25$ when a single nanofluid is replaced by a ternary nanofluid.

* Corresponding author. Department of Mechanical Engineering, Aliabad Katoul Branch, Islamic Azad University, Aliabad Katoul, Iran.
** Corresponding author. Department of Mechanical and Aeronautical Engineering, University of Pretoria, Pretoria, 0002, South Africa.
E-mail addresses: s.masoud_seyedi@aliabadiau.ac.ir (S.M. Seyyedi), mohsen.sharifpur@up.ac.za (M. Sharifpur).

https://doi.org/10.1016/j.csite.2025.105947
Received 13 March 2024; Received in revised form 21 November 2024; Accepted 23 February 2025
Available online 24 February 2025

1. Introduction

As is well known, there are three modes of heat transfer which are conduction, convection, and radiation. Convection can be classified into three categories including forced convection, free (natural) convection, and mixed convection which can occur in many industrial processes. The study of convective flow in cavities and channels has attracted the attention of researchers due to its engineering and technological applications.

1.1. Forced convection

In 2009, the laminar forced convection of a nanofluid in an annulus was numerically studied by Izadi et al. [1]. They investigated the effects of the Reynolds number on the nanofluid flow. In 2013, Nasrin et al. [2] conducted a numerical simulation of non-darcy forced convection through a channel with non-uniform heat flux in an open cavity using nanofluid. In 2017, the influence of Lorentz forces on nanofluid forced convection was investigated by Sheikholeslami and Chamkha [3] who considered the Marangoni convection. In 2018, Mohebbi et al. [4] studied the forced convection of nanofluids in an extended surface channel using the lattice Boltzmann method. In 2019, the forced convection flow in a microchannel with partial slips was conducted by Shashikumar et al. [5]. In 2024, Kada et al. [6] conducted a numerical investigation of the flow field and heat transfer of a viscoplastic fluid. They used the Bingham-Papanastasiou model to examine the flow field and forced convection heat transfer of a viscoplastic fluid between two concentric cylinders with a wavy inner surface. They found that an increase in the inertia parameter leads to a higher intensity of thermal buoyancy, thereby amplifying the heat transfer rate, especially at Re = 50.

1.2. Natural convection

In 1983, the natural convection in a square cavity was studied by de Vahl Davis [7]. Nowadays, this important work has been considered as a benchmark solution. In 1998, Yilbas et al. [8] analyzed the natural convection and entropy generation in a square cavity. In 2007, the natural convection in a differentially heated enclosure filled with a micropolar fluid was studied by Aydin and Pop [9]. In 2008, Pirmohammadi et al. [10] investigated the effect of a magnetic field on buoyancy-driven convection in a differentially heated square chamber. Also, in 2008, the effect of aspect ratio on entropy generation in a rectangular cavity with differentially heated vertical walls was studied by Ilis [11]. In 2009 Ghasemi and Aminossadati [12] analyzed the natural convection heat transfer in an inclined enclosure filled with a water-CuO nanofluid. In 2012, the buoyancy-driven flow and heat transfer in a trapezoidal cavity filled with water–Cu nanofluid were investigated by Nasrin and Parvin [13]. In 2014, Jani et al. [14] studied free convection in rectangular enclosures containing nanofluid with nanoparticles of various diameters. In 2016, Chamkha et al. [15] investigated the entropy generation and natural convection of CuO-water nanofluid in a C-shaped cavity under a magnetic field. In 2018, the MHD natural convection and entropy generation of ferrofluid in an open trapezoidal cavity partially filled with a porous medium were studied by Astanina et al. [16]. In 2018, Dogonchi et al. [17] studied the MHD natural convection of Cu/H2O nanofluid in a horizontal semi-cylinder with a local triangular heater. In 2019, the natural convection in a CuO–water nanofluid-filled cavity under the effect of an inclined magnetic field was investigated by Selimefendigil et al. [18]. In 2019, Seyyedi et al. [19,20] calculated the entropy generation in a nanofluid-filled semi-annulus cavity by considering the shape of nanoparticles. In 2020, the entropy generation in concentric annuli of 400 kV gas-insulated transmission line was investigated by Hashemi-Tilehnoee et al. [21]. In 2020, Dogonchi et al. [22] studied the influence of different shapes of nanoparticles on Cu–H2O nanofluids in a partially heated irregular wavy enclosure. In 2011, the numerical simulation of free convection of a nanofluid in L-shaped cavities was performed by Mahmoodi [23]. In 2014, Ahmed et al. [24] investigated the natural convection in a differentially heated square enclosure filled with a nanofluid. In 2017, the experimental study on natural convection of MWCNT-water nanofluids in a square enclosure was performed by Garbadeen et al. [25]. In 2019, Safwan et al. [26] studied the effect of finite wall thickness on entropy generation and natural convection in a nanofluid-filled partially heated square cavity. In 2020, the magnetohydrodynamic natural convection and entropy generation analyses inside a nanofluid-filled incinerator-shaped porous cavity with a wavy heater block were investigated by Hashemi-Tilehnoee et al. [27]. In 2018, Sheikholeslami et al. [28] studied the non-Darcy free convection of Fe3O4-water nanoliquid in a complex-shaped enclosure under the impact of uniform Lorentz force. In 2020, the entropy generation for a porous enclosure subject to a magnetic field was investigated by Seyyedi [29]. He investigated the different orientations of cardioid geometry, too. In 2019, Goodarzi et al. [30] performed a numerical simulation of natural convection heat transfer of a nanofluid within a cavity with different aspect ratios. In 2020, the entropy generation and economic analyses in a nanofluid-filled L-shaped enclosure subjected to an oriented magnetic field were studied by Seyyedi et al. [31]. In 2024, a comprehensive parametric analysis in three-dimensional permeable cavities was performed by Zineb et al. [32]. They investigated the complex interplay of factors in convective heat transfer.

1.3. Mixed convection

In 1999, Khanafer and Chamkha [33] studied the mixed convection flow in a lid-driven enclosure filled with a fluid-saturated porous medium. In 2017, the effect of a uniform inclined magnetic field on mixed convection in a lid-driven cavity was investigated by Gibanov et al. [34]. In 2019, Nazari et al. [35] performed a numerical study on mixed convection of a non-Newtonian nanofluid with porous media in a two-lid-driven square cavity. In 2015, Esfe et al. [36] studied the mixed convection fluid flow and heat transfer of a nanofluid with variable properties in a cavity with an inside quadrilateral obstacle. In 2016, the MHD mixed convection and entropy generation of the nanofluid-filled lid-driven enclosure under the influence of inclined magnetic fields

Table 1
Natural convection in cavities.

Working fluid	Without magnetic field	Horizontal magnetic field	Inclined magnetic field	Periodic magnetic field
Pure fluid (Water/air)	[7–9,11,21,44,49], [65,71–73]	[10]	[67,80]	
Micropolar fluid	[43,70,87]	[88]	[89]	
NEPCM	[92–97]	[98]	[99,100]	
Single nanofluid	[12–14,19,22–26,30,50,66,74–77]	[15–17,28,68,78,79]	[18,20,27,29,31,64,69,90]	[63]
Hybrid nanofluid	[53–56]	[57,85,86]	[81–84],	[91]
Ternary nanofluid		[61]	[62]	a

[a] The present work.

investigated by Selimefendigil et al. [37]. In 2017, Ismael et al. [38] analyzed the mixed convection in a square cavity filled with CuO-water nanofluid heated by a corner heater. In 2014, Izadi et al. [39] investigated the effects of discrete source-sink arrangements on mixed convection in a square cavity filled with nanofluid. In 2016, the MHD mixed convection and entropy generation of water–alumina nanofluid flow in a double lid driven cavity with discrete heating were studied by Hussain et al. [40]. Hashemi-Tilehnoee, and Palomo del Barrio [41], examined the cooling efficiency and heat transfer performance of a confined impinging slot jet in the mixed convection regime under a uniform magnetic field. Using numerical simulations, various fluids, including nanofluids, are evaluated for their Prandtl number effects on heat transfer and entropy generation. The results highlight the trade-off between heat transfer efficiency and entropy generation, showing that magnetic fields and high Prandtl number fluids can be optimized for effective thermal management. In a recently published work [42], the effects of electromagnetic fields and porous media were investigated for the heat transfer and entropy generation analyses in a confined impinging NEPCM-water jet cooling system within the mixed convection regime. Numerical simulations reveal that the simultaneous application of electric and magnetic fields enhances heat transfer efficiency while reducing entropy generation compared to conventional cooling methods. The findings provide valuable insights into optimizing heat transfer systems in industrial applications, particularly when using NEPCM-water suspensions and advanced electromagnetic controls. In addition to heat transfer analysis, the calculation of entropy generation is an essential step for designing thermal enclosures. The working fluid has a main effect on the thermal performance of enclosures. Conventionally, air and water have been selected as working fluids in enclosures [7,8,10,11,21,33,43,44]. But they have low thermal conductivity. In 1995, the term ‘nanofluid’ was first proposed by Choi [45]. A fluid containing nanoparticles, known as a nanofluid, has higher thermal conductivity compared to the base fluid [19]. Nowadays nanofluids have many industrial applications such as radiators [46], heating and cooling in buildings, electronics cooling, medical applications [47], and solar collectors [48]. Many papers have been published on the natural convection and entropy generation analyses in enclosures. It can be said that the oldest works on flow in a cavity were presented by Torrance et al. [49]. Khanafer et al. [50] conducted the first numerical study of the natural convection of nanofluid (Cu-water) in an enclosed square in 2003. Also, in 2024, good review research on the vehicle engine cooling system has been published by Zineb et al. [51]. Their results show that nano refrigerants outperform base liquids in warm conductivity, and the size of the nanoparticles affects this conductivity. After single nanofluids, researchers introduced hybrid nanofluids. A hybrid nanofluid consists of two types of nanoparticles dispersed in a base fluid [52]. Hybrid nanofluid has been chosen as a working fluid by some researchers [53–57]. In 2017, Gorla et al. [53] studied the heat source/sink effects on a hybrid nanofluid-filled porous cavity. In 2017, the free convection of hybrid Al_2O_3-Cu water nanofluid in a differentially heated porous cavity was investigated by Mehryan et al. [54]. In 2016, Tayebi and Chamkha [55] analyzed the free convection enhancement in an annulus between horizontal confocal elliptical cylinders using hybrid nanofluids. In 2017, the natural convection enhancement in an eccentric horizontal cylindrical annulus using hybrid nanofluids was investigated by Tayebi and Chamkha [56]. In 2109, Chamkha et al. [57] studied the magneto-hydrodynamic flow and heat transfer of a hybrid nanofluid in a rotating system among two surfaces in the presence of thermal radiation and Joule heating. In 2024, the numerical simulation of combined convection and radiation heat transfer in a hybrid nanofluid inside an open fins cavity under a magnetic field was performed by Redouane et al. [58]. They found that the highest full heat transfer ratio on the lowest warm fence occurs without magnetic field ($Ha = 0$). Recently, trihybrid nanofluids (ternary nanofluids) have attracted the attention of researchers. They are formed by suspending three types of nanoparticles (such as Cu, Al_2O_3, and Fe_3O_4) with different physical and chemical bonds into a base fluid (such as water, glycol, and mineral oil). Ternary nanofluid is a novel class of working fluids with excellent heat transfer properties that can be controlled by their stabilities [59]. Ternary nanofluids have shown better heat conduction than mono and hybrid nanofluids [60–62]. Some of the most important published papers on natural convection are introduced in Table 1.

According to Table 1, no work has been done on the periodic magnetic field of ternary nanofluid. Some excellent comprehensive review articles on the natural convection in enclosures are given by Yang [101], Ostrach [102], Fusegi and Hyun [103], Das et al. [104], Giwa et al. [105], and Wang et al. [106].

According to the literature review, this study investigates the consequences of a periodic magnetic field on naturally occurring convection and entropy formation in a square-enclosed space filled with a ternary nanofluid (Cu-Al_2O_3-Fe_3O_4-water).

2. Definition of the problem

Here, a square enclosure filled with a ternary nanofluid is considered where the working fluid is altered by an external periodic magnetic field. The magnetic field is applied as a sinusoidal function of the y coordinate. The left and right walls are maintained at

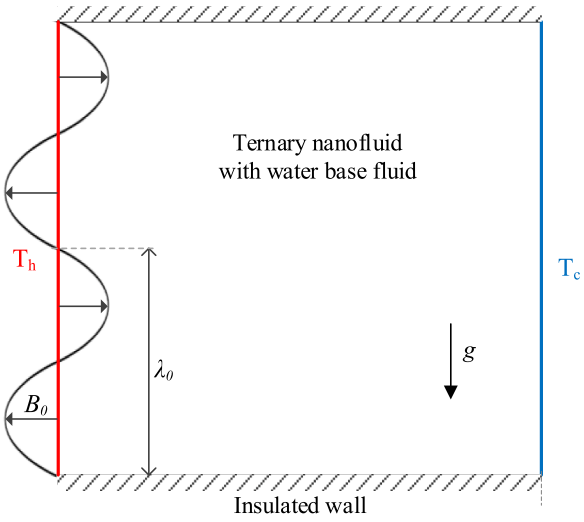

Fig. 1. Schematic view of the considered problem.

Table 2
Relations for calculating the ternary nanofluid properties.

Properties	Computational relations for ternary nanofluids
Ternary nanofluid	$\phi = \sum_{j=1}^{3} \phi_j$
Dynamic Viscosity	$\mu_{tnf} = \frac{1}{\phi}\sum_{j=1}^{3}\left(\mu_{nf}\phi\right)_j$ where $\left(\mu_{nf}\right)_j = \frac{\mu_f}{\left(1-\phi_j\right)^{2.5}}$
Density	$\rho_{tnf} = \rho_f(1-\phi) + \sum_{j=1}^{3}\left(\rho_j\phi_j\right)$
Heat capacity	$\left(\rho c_p\right)_{tnf} = \left(\rho c_p\right)_f(1-\phi) + \sum_{j=1}^{3}\left(\rho c_p\phi\right)_j$
Thermal Expansion	$\left(\rho\beta\right)_{tnf} = \left(\rho\beta\right)_f(1-\phi) + \sum_{j=1}^{3}\left(\rho\beta\phi\right)_j$
Thermal Conductivity	$k_{tnf} = \frac{1}{\phi}\sum_{j=1}^{3}\left(k_{nf}\phi\right)_j$ where $\frac{\left(k_{nf}\right)_j}{k_f} = \frac{k_j + (m_j-1)k_f - (m_j-1)\phi_j(k_f-k_j)}{k_j + (m_j-1)k_f + \phi_j(k_f-k_j)}$
Electrical conductivity	$\sigma_{tnf} = \frac{1}{\phi}\sum_{j=1}^{3}\left(\sigma_{nf}\phi\right)_j$ where $\frac{\left(\sigma_{nf}\right)_j}{\sigma_f} = 1 + \frac{3\left(\frac{\sigma_j}{\sigma_f}-1\right)\phi_j}{\left(\frac{\sigma_j}{\sigma_f}+2\right) - \left(\frac{\sigma_j}{\sigma_f}-1\right)\phi_j}$

constant temperatures T_h and T_c $(T_c < T_h)$, respectively, while the two other walls are thermally insulated. The schematic view of the considered problem is shown in Fig. 1.

3. Mathematical model

3.1. Basic governing equations

In order to analysis the natural convective heat transfer, it is assumed that the flow is steady, two-dimensional, laminar and incompressible. The viscous dissipation, radiation, Joule heating and induced electric current are neglected. The period and amplitude of the periodic magnetic field are λ_0 and B_0, respectively. The periodic magnetic field can be obtained as follows [63]:

$$B = B_0 \sin\left(\frac{\pi y}{\lambda_0}\right) \tag{1}$$

The governing equations (mass, momentum, and energy conservations) for ternary nanofluid may be found as follows by employing the Boussinesq approximation [20]:

$$\frac{\partial u}{\partial x} + \frac{\partial v}{\partial y} = 0 \tag{2}$$

$$\rho_{tnf}\left(u\frac{\partial u}{\partial x} + v\frac{\partial u}{\partial y}\right) = -\frac{\partial P}{\partial x} + \mu_{tnf}\left(\frac{\partial^2 u}{\partial x^2} + \frac{\partial^2 u}{\partial y^2}\right) \tag{3}$$

$$\rho_{tnf}\left(u\frac{\partial v}{\partial x}+v\frac{\partial v}{\partial y}\right)=-\frac{\partial P}{\partial y}+\mu_{tnf}\left(\frac{\partial^2 v}{\partial x^2}+\frac{\partial^2 v}{\partial y^2}\right)-\sigma_{tnf}B_0^2\sin^2\left(\frac{\pi y}{\lambda_0}\right)v+g(\rho\beta)_{tnf}(T-T_c) \tag{4}$$

$$(\rho c_p)_{tnf}\left(u\frac{\partial T}{\partial x}+v\frac{\partial T}{\partial y}\right)=k_{tnf}\left(\frac{\partial^2 T}{\partial x^2}+\frac{\partial^2 T}{\partial y^2}\right) \tag{5}$$

Respective relations for calculating the ternary nanofluid properties are given in Table 2.

3.2. Non dimensional form of governing equations

The vorticity (ω), stream function (ψ), and dimensionless variables in this work are defined as follows:

$$u=\frac{\partial \psi}{\partial y}, v=-\frac{\partial \psi}{\partial x} \text{ and } \quad \omega=\frac{\partial v}{\partial x}-\frac{\partial u}{\partial y} \tag{6}$$

$$\mathrm{X}=\frac{x}{L}, \mathrm{Y}=\frac{y}{L}, \theta=\frac{T-T_c}{T_h-T_c}, \Omega=\frac{\omega L^2}{\alpha_f} \text{ and } \quad \Psi=\frac{\psi}{\alpha_f} \tag{7}$$

Thus, using Eqs. (1), (6) and (7), Eqs. (2)–(5) can be rewritten in the non-dimensional forms, as follows:

$$\frac{\partial^2 \Psi}{\partial \mathrm{X}^2}+\frac{\partial^2 \Psi}{\partial \mathrm{Y}^2}=-\Omega \tag{8}$$

$$\left[\frac{\partial \Omega}{\partial \mathrm{X}}\frac{\partial \Psi}{\partial \mathrm{Y}}-\frac{\partial \Omega}{\partial \mathrm{Y}}\frac{\partial \Psi}{\partial \mathrm{X}}\right]=\frac{\mu_{tnf}/\mu_f}{\rho_{tnf}/\rho_f}\mathrm{Pr}\left(\frac{\partial^2 \Omega}{\partial \mathrm{X}^2}+\frac{\partial^2 \Omega}{\partial \mathrm{Y}^2}\right)+\frac{\beta_{tnf}}{\beta_f}\mathrm{Ra}\,\mathrm{Pr}\frac{\partial \theta}{\partial \mathrm{X}}+\frac{\sigma_{tnf}/\sigma_f}{\rho_{nf}/\rho_f}\mathrm{Ha}^2\,\mathrm{Pr}\frac{\partial^2 \Psi}{\partial \mathrm{X}^2}\sin^2\left(\frac{\pi Y}{\lambda}\right) \tag{9}$$

$$\left[\frac{\partial \Psi}{\partial \mathrm{Y}}\frac{\partial \theta}{\partial \mathrm{X}}-\frac{\partial \Psi}{\partial \mathrm{X}}\frac{\partial \theta}{\partial \mathrm{Y}}\right]=\frac{\alpha_{tnf}}{\alpha_f}\left(\frac{\partial^2 \theta}{\partial \mathrm{X}^2}+\frac{\partial^2 \theta}{\partial \mathrm{Y}^2}\right) \tag{10}$$

In Eq. (9), Pr , Ha , *Ra* and λ are the Prandtl number, the Hartmann number, Rayleigh number, and period number respectively, that are expressed as follows:

$$\mathrm{Pr}=\frac{\nu_f}{\alpha_f}, \mathrm{Ra}=\frac{g\beta_f L^3(T_h-T_c)}{\nu_f \alpha_f}, \mathrm{Ha}=B_0 L\sqrt{\frac{\sigma_f}{\rho_f \nu_f}}, \lambda=\frac{\lambda_0}{L} \tag{11}$$

Also,

$$\alpha_{tnf}=\frac{k_{tnf}}{(\rho c_p)_{tnf}} \tag{12}$$

Fig. 1 depicts the boundary conditions, which are:
$\Psi=0$ on all solid boundaries $\frac{\partial \theta}{\partial n}=0$ on two other walls $\theta=1.0$ on the left (hot) wall $\theta=0.0$ on the right (cold) wall (13).
The Nusselt numbers (local and average) over the heated wall can be stated as follows:

$$\mathrm{Nu}_{local}=-\left(\frac{k_{tnf}}{k_f}\right)\left(\frac{\partial \theta}{\partial \mathrm{X}}\right)_{X=0} \tag{14}$$

$$\mathrm{Nu}_{\mathrm{ave}}=\frac{1}{L}\int_0^L \mathrm{Nu}_{local}(y)dy=\int_0^1 \mathrm{Nu}_{local}(Y)dY \tag{15}$$

3.3. Entropy generation

Energy system design can be completed using entropy generation calculation. The rate of entropy generation can be evaluated by Eq. (16) [29]:

$$\dot{S}_{\mathrm{gen}}=\frac{k_{tnf}}{T_0^2}\left[\left(\frac{\partial T}{\partial x}\right)^2+\left(\frac{\partial T}{\partial y}\right)^2\right]+\frac{\mu_{tnf}}{T_0}\left[2\left(\frac{\partial u}{\partial x}\right)^2+2\left(\frac{\partial v}{\partial y}\right)^2+\left(\frac{\partial u}{\partial y}+\frac{\partial v}{\partial x}\right)^2\right]+\frac{\sigma_{tnf}B_0^2}{T_0}\sin^2\left(\frac{\pi y}{\lambda_0}\right)v^2 \tag{16}$$

Three terms make up the local entropy generation equation (16): local entropy generation resulting from heat transfer, local entropy generation resulting from viscous dissipation, and local entropy generation resulting from the influence of the magnetic field. The local entropy generation $N_{\mathrm{L,gen}}$ equation can be constructed in the following non-dimensional manner [29]:

$$N_{L,gen}=\frac{\dot{S}_{gen}}{\left[\left(\frac{k_f}{T_0^2}\right)\left(\frac{\Delta T}{L}\right)^2\right]}=\frac{k_{tnf}}{k_f}\left[\left(\frac{\partial\theta}{\partial X}\right)^2+\left(\frac{\partial\theta}{\partial Y}\right)^2\right]+\frac{\mu_{tnf}}{\mu_f}\Phi_f\left[4\left(\frac{\partial^2\Psi}{\partial X\partial Y}\right)^2+\left(\frac{\partial^2\Psi}{\partial Y^2}-\frac{\partial^2\Psi}{\partial X^2}\right)^2\right]+\frac{\sigma_{tnf}}{\sigma_f}Ha^2\sin^2\left(\frac{\pi Y}{\lambda}\right)\Phi_f\left(\frac{\partial\Psi}{\partial X}\right)^2 \tag{17}$$

where Φ_f is the irreversibility distribution ratio and it is defined as follows:

$$\Phi_f=\frac{\mu_f T_0}{k_f}\left(\frac{\alpha_f}{L\Delta T}\right)^2 \tag{18}$$

where ΔT is the temperature difference in the cavity $(\Delta T=T_h-T_c)$ and $(T_0=(T_h+T_c)/2)$ is the mean temperature.

One possible rewrite of Eq. (17) is given as:

$$N_{L,gen}=N_{L,HT}+N_{L,FF}+N_{L,MF} \tag{19}$$

Where $N_{L,HT}$, $N_{L,FF}$ and $N_{L,MF}$ are the local entropy generation number due to heat transfer irreversibility, fluid friction irreversibility and magnetic field irreversibility, respectively. Therefore, one can have

$$N_{L,HT}=\frac{k_{tnf}}{k_f}\left[\left(\frac{\partial\theta}{\partial X}\right)^2+\left(\frac{\partial\theta}{\partial Y}\right)^2\right] \tag{20}$$

$$N_{L,FF}=\frac{\mu_{tnf}}{\mu_f}\Phi_f\left[4\left(\frac{\partial^2\Psi}{\partial X\partial Y}\right)^2+\left(\frac{\partial^2\Psi}{\partial Y^2}-\frac{\partial^2\Psi}{\partial X^2}\right)^2\right] \tag{21}$$

$$N_{L,MF}=\frac{\sigma_{tnf}}{\sigma_f}Ha^2\sin^2\left(\frac{\pi Y}{\lambda}\right)\Phi_f\left(\frac{\partial\Psi}{\partial X}\right)^2 \tag{22}$$

By integrating the locally produced entropy over the system volume, the total entropy production may be found:

$$N_{T,HT}=\int_V N_{L,HT}\,dV \tag{23}$$

$$N_{T,FF}=\int_V N_{L,FF}\,dV \tag{24}$$

$$N_{T,MF}=\int_V N_{L,MF}\,dV \tag{25}$$

The sum of the quantities in Eqs. 23–25 is N_{gen} referred to as the entropy generation number.

$$N_{gen}=N_{T,HT}+N_{T,FF}+N_{T,MF} \tag{26}$$

3.4. Bejan number

The Bejan number (local and average) is defined, respectively as follows [20]:

$$Be_L=N_{L,HT}/N_{L,gen} \tag{27}$$

$$Be_{ave}=\frac{\int_A Be_L(X,Y)dA}{\int_A dA} \tag{28}$$

3.5. Ecological Coefficient of Performance (ECOP)

In 2019, Seyyedi et al. [19] introduced the "Ecological Coefficient of Performance" (ECOP) as a standard for assessing cavities' thermal performance.

$$ECOP=\frac{Nu_{ave}}{N_{gen}} \tag{29}$$

4. Numerical procedure

This paper employs the control volume finite element method (CVFEM). Saabas and Baliga introduced this approach [107]. The underlying equations are handled by extending a FORTRAN code.

Table 3
The impact of grid size on the average Nusselt number and entropy generation.

Mesh	81 × 81	91 × 91	101 × 101	111 × 111	121 × 121	131 × 131
$\lvert\Psi_{max}\rvert$	10.31	10.21	10.135	10.07	10.02	9.98
Nu_{ave}	4.8078	4.7967	4.7849	4.7732	4.7621	4.7516
N_{gen}	33.22	33.43	33.6220	33.7927	33.9442	34.0780

Table 4
Assessment of the current findings with previous research for Nu_{ave} and N_{gen}

Nu_{ave}					N_{gen}		
Ra	Khanafer et al. [50]	Zadravec et al. [43]	Aydin and Pop [9]	Present code	Ilis et al. [11]	Shavik et al. [44]	Present code
10^3	1.118	1.118	1.118	1.118	1.20	1.15	1.134
10^4	2.245	2.263	2.234	2.246	–	–	–
10^5	4.522	4.540	4.486	4.553	23.50	23.27	23.20
10^6	8.826	8.742	8.945	8.761	–	–	–

Table 5
The values of Nu_{ave} for various values of Hartmann number ($Ra = 10^4$ and $Ra = 10^5$) with $Pr = 0.733$

Ra	Ha	Pirmohammadi et al. [10]	Present study		Pirmohammadi et al. [10]	Present study	
		$\lvert\Psi_{max}\rvert$		Error (%)	Nu_{ave}		Error (%)
10^4	0	5.05	5.07	0.47	2.29	2.249	1.79
	10	3.35	3.42	2.1	1.97	1.934	1.83
	50	0.47	0.49	4.2	1.06	1.040	1.89
	100	0.12	0.124	3.3	1.02	1.004	1.57
10^5	0	9.75	9.74	0.1	4.62	4.571	1.06
	25	6.41	6.54	2.03	3.51	3.470	1.14
	100	1.14	1.19	4.4	1.37	1.346	1.75

Table 6
Thermophysical characteristics of water and nanoparticles [63,89,108].

Symbol	Name	$\rho(kg/m^3)$	$c_p(J/kgK)$	$k(W/mK)$	$\beta_T\ (1/K)$	$\sigma(\mu S/cm)$
ϕ_1	Cu	8933	385	401	1.67×10^{-5}	5.96×10^7
ϕ_2	Alumina (Al_2O_3)	3970	765	40	8.5×10^{-6}	1×10^{-10}
ϕ_3	Ferrofluid (Fe_3O_4)	5200	670	6	1.3×10^{-5}	2.5×10^3
	Pure water	997.1	4179	0.613	21×10^{-5}	0.05

4.1. CVFEM

Two popular classes of methods are (i) Finite Difference Methods (FDM) and (ii) Finite Element Methods (FEM). A distinction between the methods is the nature of the nodal locations. To overcome some drawbacks of these two methods, the Control Volume Finite Difference Method (CVFDM) was developed. In this approach, control volumes are created around the node points on a structured grid. An attractive feature of this method is that it has a direct connection to the physics of the system. However, the CVFDM is still subject to the geometric constraints of the basic FDM. Then, the CVFEM was developed to overcome this drawback. The key feature to recognize is that control volumes can also be constructed around the node points on an unstructured finite element mesh that conforms to an arbitrarily shaped domain. In summary, CVFEM is a numerical method that combines the advantages of FEM and Finite Volume Methods (FVM).

4.2. The grid test

The grid sizes of 81 × 81, 91 × 91, 101 × 101, 111 × 111, 121 × 121 and 131 × 131 have been evaluated to guarantee the grid-independent solution for the case of $Ra = 10^5$ ، $Ha = 25$ ، $\lambda = 0.25$ ، $Pr = 6.2$ ، $\phi = 0.05$ ، $m = 3$ and $\Phi = 10^{-4}$. The result for the average Nusselt number (Nu_{ave}), the maximum absolute value of the stream function $\lvert\Psi_{max}\rvert$, and the entropy generation number (N_{gen}) are shown in Table 3. The relative errors between the last two columns for values of $\lvert\Psi_{max}\rvert$, Nu_{ave} and N_{gen} are −0.4 %, −0.22 % and 0.39 %, respectively. Consequently, based on this data, 121 × 121 has been chosen as the gird size.

Table 7
The default values of the nondimensional parameters.

Ra	Ha	λ	P r	ϕ_1	ϕ_2	ϕ_3	m	Φ
10^5	25	0.25	6.2	0.02	0.02	0.01	3	10^{-4}

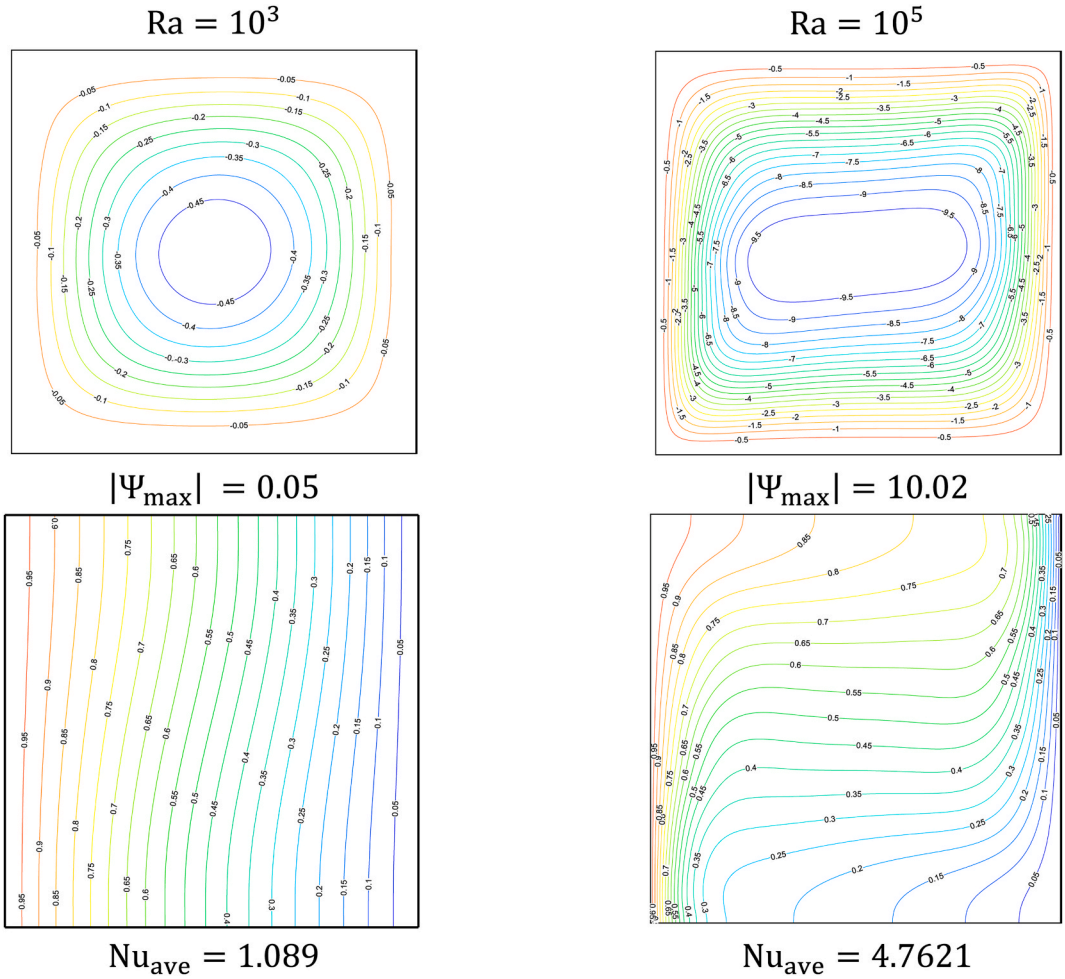

Fig. 2. (Ψ) and (θ) for two values of Rayleigh number.

4.3. Validation

The present FORTRAN code is validated by comparing the obtained results with other work reported in the literature. Tables 4 and 5 demonstrate a high degree of consistency between the outcomes of Refs [9–11,43,44,50] and the current computations.

5. Results and discussion

The CVFEM is used to calculate the naturally occurring convection heat transfer and entropy formation in a square enclosure occupied with a ternary nanofluid. Table 6 displays the thermophysical properties of based fluids and nanoparticles. Also, the values of the shape factor for various nanoparticles can be found in Refs. [31,64]. Table 7 presents the default values of the nondimensional parameters for calculations unless the new values are stated.

Fig. 2 demonstrates the isotherms and the streamlines at Ra $= 10^3$ and Ra $= 10^5$. The maximum absolute value of stream function ($|\Psi_{max}|$) can be considered as a measure of the intensity of natural convection in the cavity. The values of $|\Psi_{max}|$ are 0.05 and 10.02 for Ra $= 10^3$ and Ra $= 10^5$, respectively. This indicates that the flow occurs more rapidly as the Rayleigh number increases. Also, the shape of the isotherms shows that heat transfer conduction mode is dominated by convection mode when the Rayleigh number increases. At Ra $= 10^3$ isotherms are parallel to vertical walls but at Ra $= 10^5$ they are distorted. The values of average Nusselt number

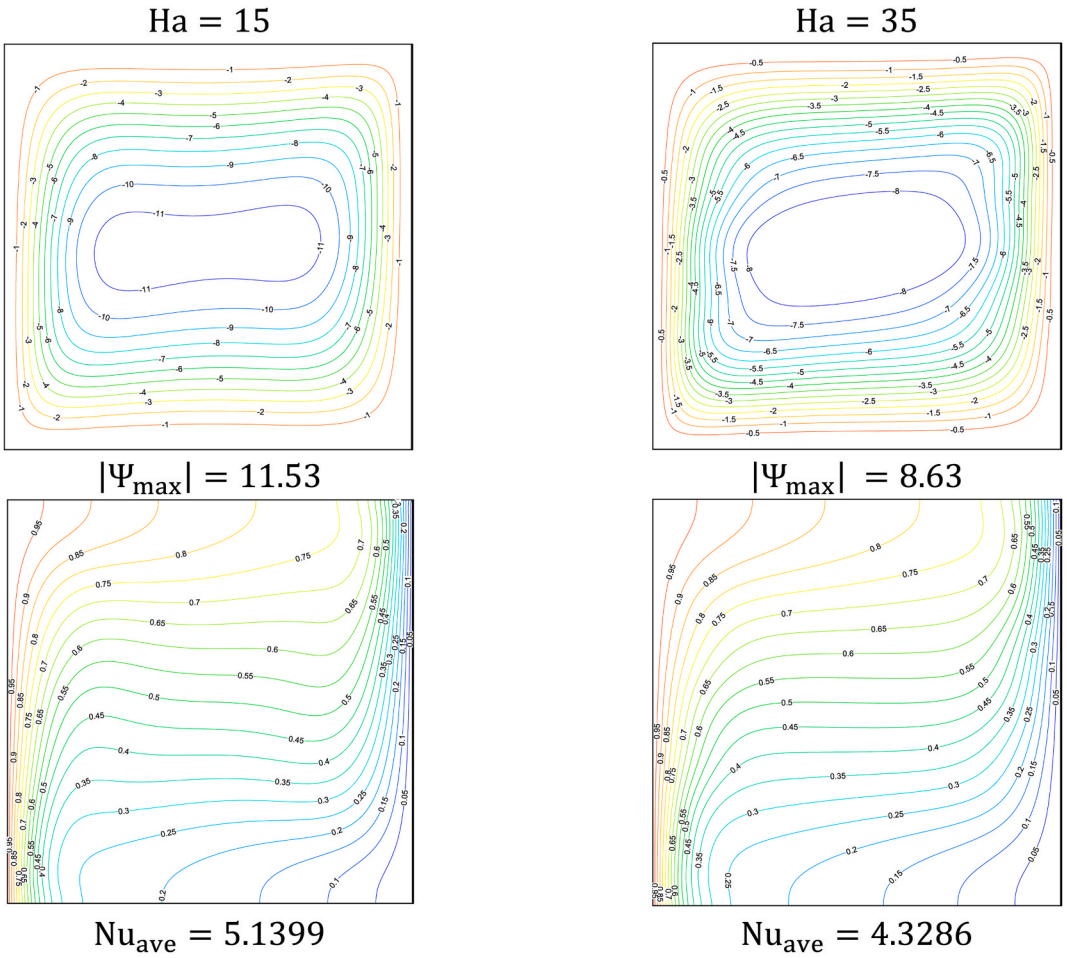

Fig. 3. (Ψ) and (θ) for two values of Hartmann number.

(Nu_{ave}) indicate this issue where they are 1.089 and 4.7621 for $Ra = 10^3$ and $Ra = 10^5$, respectively.

Fig. 3 depicts the impact of a magnetic field on the streamlines and the isotherms. The figure discovers that an increment in Hartmann number extremely diminishes the strength of the vortices circulating inside the enclosure. The value of $|\Psi_{max}|$ decreases from 11.53 to 8.63 (25.2 % decrease) when *Ha* increases from 15 to 35. Also, the value of Nu_{ave} decreases from 5.1399 to 4.3286 (15.8 % decrease) when *Ha* increases from 15 to 35. Therefore, the heat transfer rate of natural convection decreases with ascending *Ha* because the velocity of fluid flow decreases.

Fig. 4 presents the Nu_{ave}, N_{gen}, Be_{ave}, and the ECOP versus the period number (λ) for three values of Hartmann number. Fig. 4(a) shows that there is a maximum value for Nu_{ave} when the period number is changed for each Hartmann number. For example, the highest value of Nu_{ave} occurs at $\lambda = 0.7$. The reason is that the intensity of the magnetic field decreases at $\lambda = 0.7$. Also, the value of Nu_{ave} decreases from 4.7860 to 4.3948 (8.2 % reducing) for the case when *Ha* rises from 25 to 35 at $\lambda = 0.7$. Fig. 4(b) discovers that the N_{gen} firstly decreases, attains to a minimum value and then increases when the period number enhances. The minimum value of N_{gen} occurs at $\lambda = 0.6$. For example, the value of N_{gen} decreases from 34.066 to 32.902 (3.4 % decreasing) when λ increases from 0.1 to 0.6 while it increases from 32.902 to 35.895 (9.1 % rising) when λ upsurges from 0.6 to 1.0 at $Ha = 25$. Also, the figure displays that the value of N_{gen} intensifies from 32.902 to 33.601 (2.1 % increasing) when *Ha* propagates from 25 to 35 at $\lambda = 0.6$. Fig. 4(c) shows that the range of changes in the Be_{ave} for $Ha = 35$ is greater than the range of changes in the two other cases. For example, the value of Be_{ave} decreases from 0.274 to 0.221(19.3 % decreasing) for $Ha = 35$ while it only decreases from 0.26 to 0.252 (3.1 % reducing) for $Ha = 15$ when λ raises from 0.1 to 1.0. Fig. 4(d) illustrates that there is the highest value for ECOP at each Hartmann number. The highest values of ECOP occur at $\lambda = 0.6$. They are 0.1662, 0.1450 and 0.1298, for $Ha = 15$, $Ha = 25$ and $Ha = 35$, respectively. This is because the amount of heat transfer increases while the amount of entropy generation decreases at $\lambda = 0.6$. The graph reveals that the ECOP values drop with a rising Hartmann number for each value of λ.

Fig. 5 depicts the effects of period number (λ) on the isotherms and the streamlines. This figure indicates that the value of $|\Psi_{max}|$ ascends from 6.31 to 6.41 (1.6 % ascending) whereas the value of Nu_{ave} descends from 4.3286 to 3.5014 (19.1 % descending) when λ increases from 0.1 to 0.25. Indeed, the intensity of the magnetic field increases with increasing the λ.

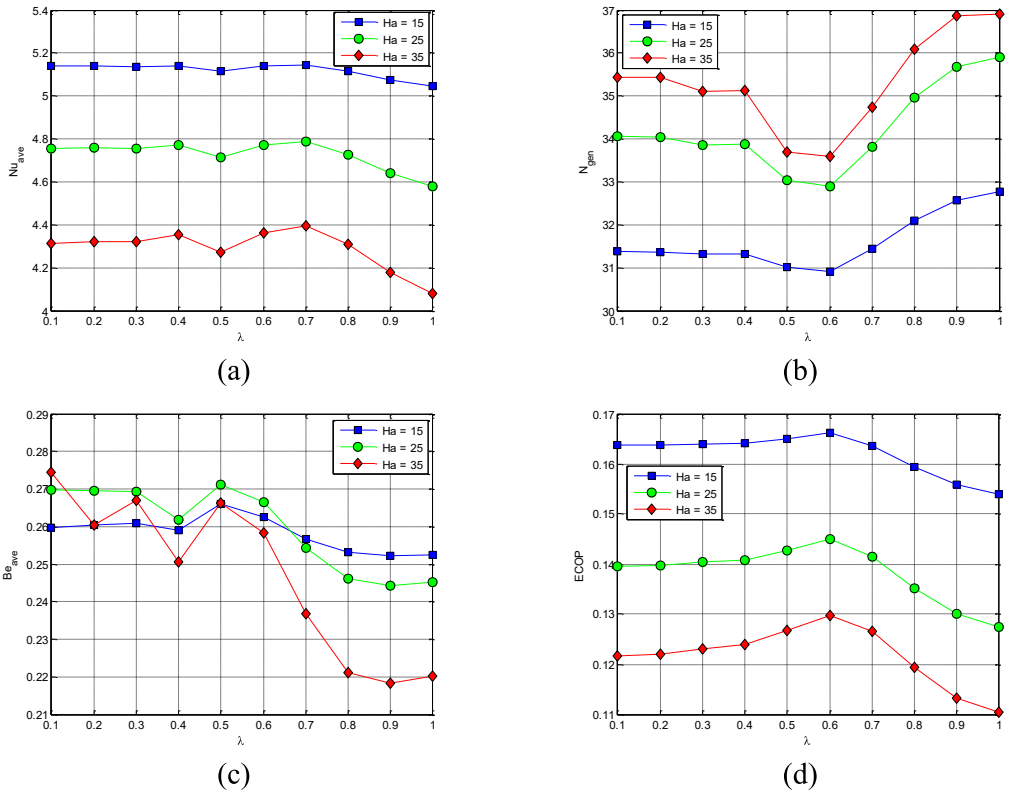

Fig. 4. The variations of Nu_{ave}, N_{gen} , Be_{ave} and ECOP versus λ for different values of Hartmann number.

Fig. 6 presents the Nu_{ave}, the N_{gen} , Be_{ave} and the ECOP against the Rayleigh number (Ra) for three values of the Hartmann number. The shape indicates that the values of Nu_{ave} and N_{gen} increase with the Ra while the values of Be_{ave} and ECOP decreases as Ra increases. For example, the values of Nu_{ave} and N_{gen} increase from 1.4529 to 1.9356 to 3.6646 and 15.983, respectively when Ra goes up from 5×10^3 to 5×10^4 at Ha $= 25$. Also, the values of Be_{ave} and ECOP decrease from 0.7609 to 0.7506 to 0.3438 and 0.2293, respectively when Ra goes up from 5×10^3 to 5×10^4 at Ha $= 25$. A decreasing average Bejan number indicates that entropy generation due to heat transfer decreases with respect to the total entropy generation.

Fig. 7 demonstrates the values of Nu_{ave} and N_{gen} for various values of period number at three different values of Ferrofluid (Fe_3O_4) nanoparticles. The chart reveals that the values of Nu_{ave} and N_{gen} rise with increasing ϕ_3 for each value of λ. For example, the values of Nu_{ave} and N_{gen} increase from 4.6883 to 32.164 to 4.7512 and 34.06, respectively, when ϕ_3 goes up from 0 to 0.02 at $\lambda = 0.50$.

Fig. 8 presents a comparison between the values of N_{gen} and ECOP for single, hybrid, and ternary nanofluid at two different values of Hartmann number. As it can be seen, the lowest value of N_{gen} and the highest value of ECOP corresponds to a ternary nanofluid for each Hartmann number. For example, the value of N_{gen} decreases from 40.75 to 33.94 (16.7 % decrease) while the value of ECOP increases from 0.1251 to 0.1402 (12.1 % increase) at Ha $= 25$ when a single nanofluid is replaced by a ternary nanofluid. It is worth noting that in all cases $\phi = 0.05$.

Fig. 9 presents the contribution of the heat transfer $(N_{T,HT})$, the fluid friction $(N_{T,FF})$ and the magnetic field $(N_{T,MF})$ in the total entropy generation number for two different values of the Hartmann number. The figure discovers that the $N_{T,FF}$ decreases from 61 % to 31 % while the $N_{T,MF}$ increases from 23 % to 57 % when Hartmann number goes up from 15 to 35. This is due to an increase in the strength of the magnetic field and a decrease in the velocity of the fluid flow.

Fig. 10 depicts the variation of the local Nusselt number (Nu_{Local}) along the hot wall for three different values of period number. For every value of λ, the figure discovers that Nu_{Local} has the highest value close to the base of the vertical hot wall.

Fig. 11 demonstrates the variation of Nu_{ave} and N_{gen} versus α_λ where it is defined as follows:

$$\alpha_\lambda = \frac{\phi_1}{\phi_1 + \phi_2} \text{ where } 0.5 < \alpha_\lambda < 1, \phi_1 + \phi_2 = 0.04, \phi_3 = 0.01 \tag{30}$$

In the other words, ϕ_1 and ϕ_2 are between 0.02 and 0.04. The figure demonstrates that Nu_{ave} and N_{gen} ascend with ascending α_λ. Two correlations are proposed for Nu_{ave} and N_{gen} that were obtained by curve fitting in MATLAB software and their coefficients are given in Table 8.

Subsequently, two relationships between Nu_{ave} and N_{gen} are suggested as a function of *Ha*, ϕ and λ at Ra $= 10^5$ which are given by:

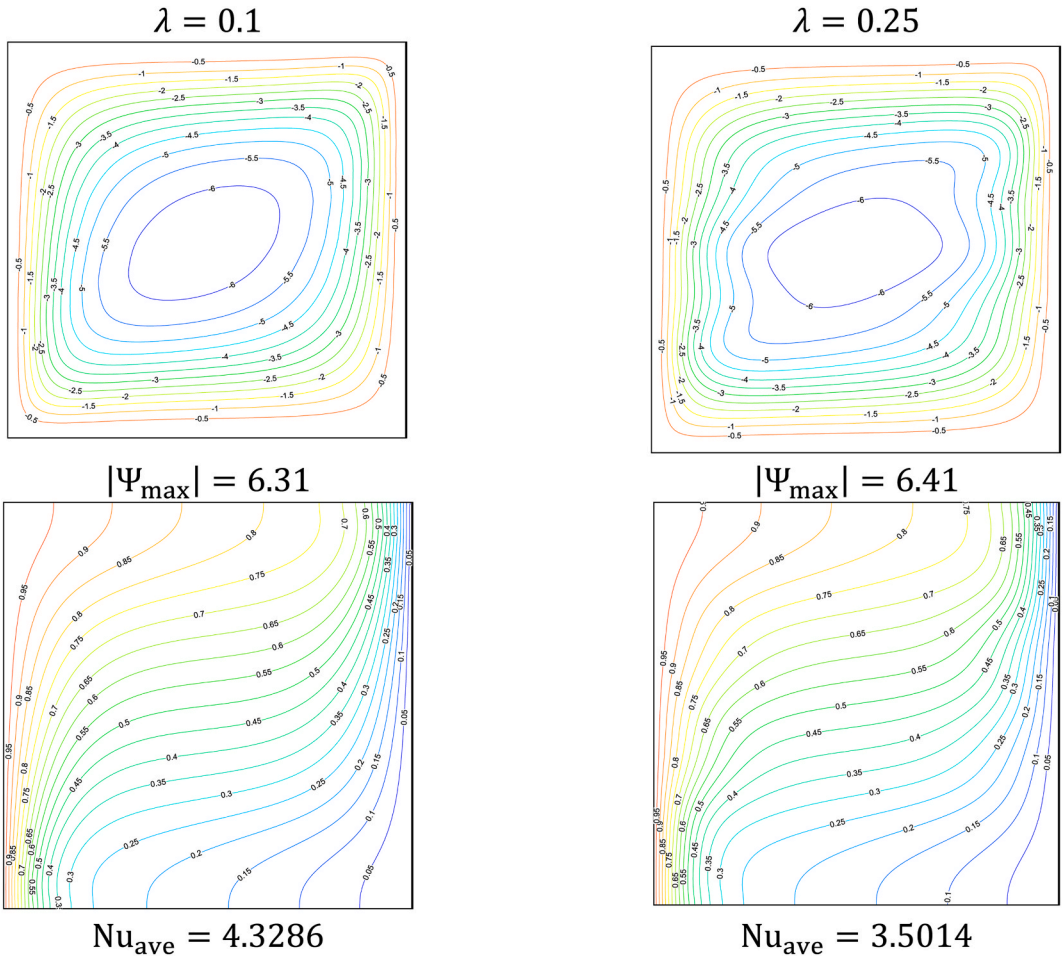

Fig. 5. (Ψ) and (θ) for two values of period number.

$$\mathrm{Nu_{ave}} = 5.31564 - 0.031527 \times \mathrm{Ha} - 0.29942 \times \lambda + 10.14876 \times \phi + 2.33333 \times 10^{-3} \times \mathrm{Ha} \times \lambda - 4.08000 \times 10^{-3} \times \mathrm{Ha} \times \phi - 4.44444 \times 10^{-3} \times \lambda \times \phi - 1.28276 \times 10^{-4} \times \mathrm{Ha}^2 + 0.12804 \times \lambda^2 - 36.19636 \times \phi^2 \quad (31)$$

$$\mathrm{N_{gen}} = 22.52789 + 0.28904 \times \mathrm{Ha} - 8.25151 \times \lambda + 308.63904 \times \phi + 0.035689 \times \mathrm{Ha} \times \lambda + 1.40560 \times \mathrm{Ha} \times \phi + 10.97778 \times \lambda \times \phi - 4.72844 \times 10^{-3} \times \mathrm{Ha}^2 + 8.06779 \times \lambda^2 - 3999.63636 \times \phi^2 \quad (32)$$

With $R^2 = 0.9814$ and $R^2 = 0.9789$ for Eqs. (31) and (32), respectively. It should be mentioned that these equations are valid for, $0.1 < \lambda < 1$, $0 < \mathrm{Ha} < 50$ and $0 < \phi < 0.05$.

6. Conclusion

In this work, the effects of the periodic magnetic field on the entropy generation and natural convection inside a cavity filled with ternary nanofluid were investigated. The ternary nanofluid (Cu-Al_2O_3-Fe_3O_4-water) was chosen as a working fluid. The key findings can be paraphrased as follows:

1. The value of $|\Psi_{max}|$ increases from 0.05 to 10.02 (200 times) and the value of Nu_{ave} increases from 1.089 to 4.7621 (4.4 times) when the value of Ra goes up from 10^3 to 10^5 (Fig. 2).
2. The values of $|\Psi_{max}|$ and Nu_{ave} decrease 25.2 % and 15.8 %, respectively when *Ha* increases from 15 to 35 (Fig. 3).
3. The maximum value of Nu_{ave} and the smallest value of N_{gen} occur at $\lambda = 0.7$ and at $= 0.6$, respectively (Fig. 4).
4. The value of Be_{ave} decreases 19.3 % and 3.1 % at Ha $= 35$ and Ha $= 15$, respectively when λ increases from 0.1 to 1.0 (Fig. 4).
5. The maximum values of ECOP are 0.1662, 0.1450, and 0.1298, for Ha $= 15$, Ha $= 25$ and Ha $= 35$, respectively (Fig. 4).

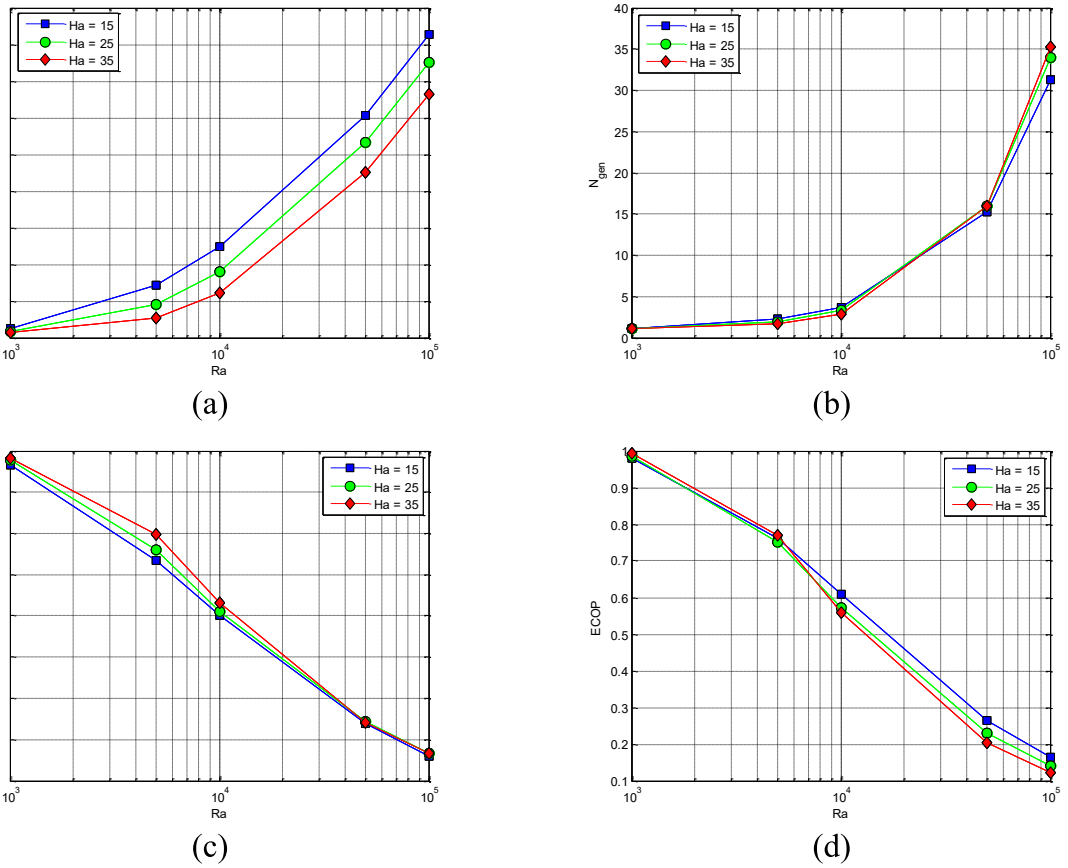

Fig. 6. The variations of Nu_{ave}, N_{gen} , Be_{ave} and ECOP versus Ra for different values of Hartmann number.

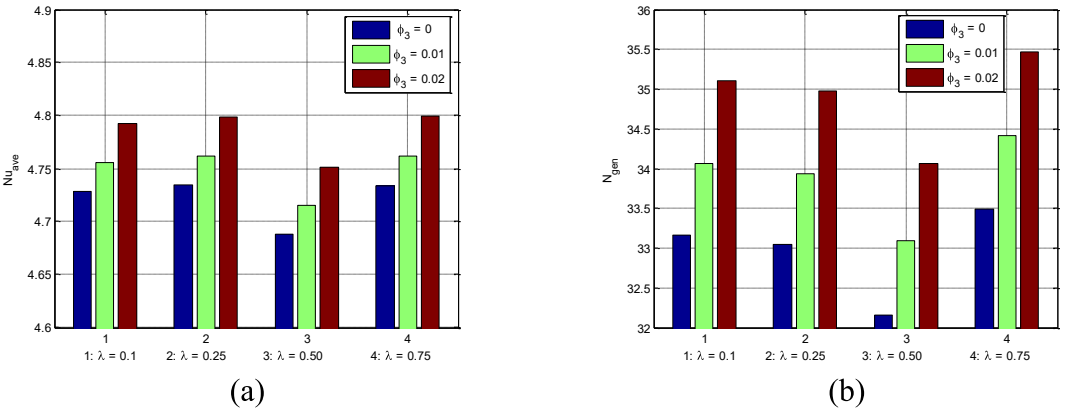

Fig. 7. The values of Nu_{ave} and N_{gen} for various values of period number at three different values of ϕ_3

6. The value of Nu_{ave} descends 19.1 % when λ increases from 0.1 to 0.25 (Fig. 5).
7. The values of Nu_{ave} and N_{gen} increase 2.52 times and 8.26 times, respectively when Ra goes up from 5×10^3 to 5×10^4 at Ha = 25 (Fig. 6).
8. The values of Nu_{ave} and N_{gen} increase by 1.3 % and 5.9 % respectively, when ϕ_3 goes up from 0 to 0.02 at $\lambda = 0.50$ (Fig. 7).
9. The value of N_{gen} decreases by 16.7 % while the value of ECOP increases by 12.1 % at Ha = 25 when a single nanofluid is replaced by a ternary nanofluid (Fig. 8).
10. The $N_{T,HT}$ decreases from 16 % to 12 % while the $N_{T,MF}$ increases from 23 % to 57 % when the Hartmann number goes up from 15 to 35 (Fig. 9).

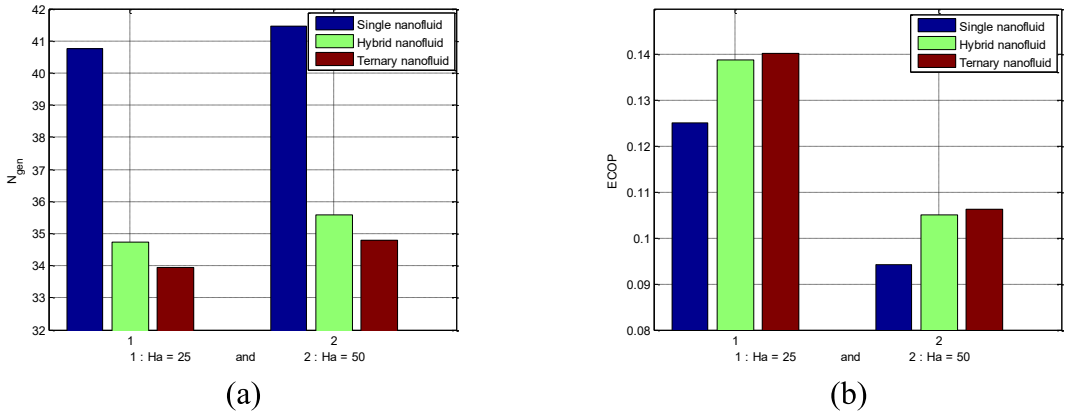

Fig. 8. The values of N_{gen} and ECOP for single, hybrid, and ternary nanofluids at Ha = 0 and Ha = 20

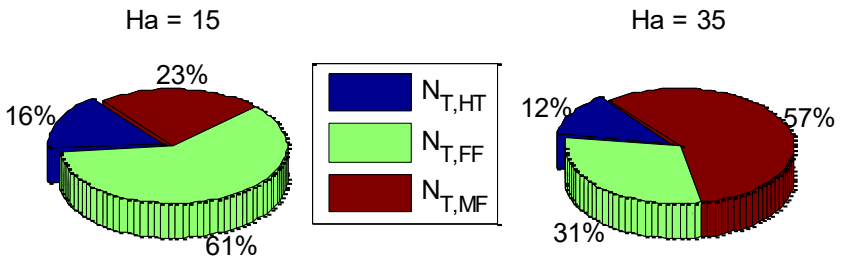

Fig. 9. Contribution of components in the N_{gen} at two values of Ha

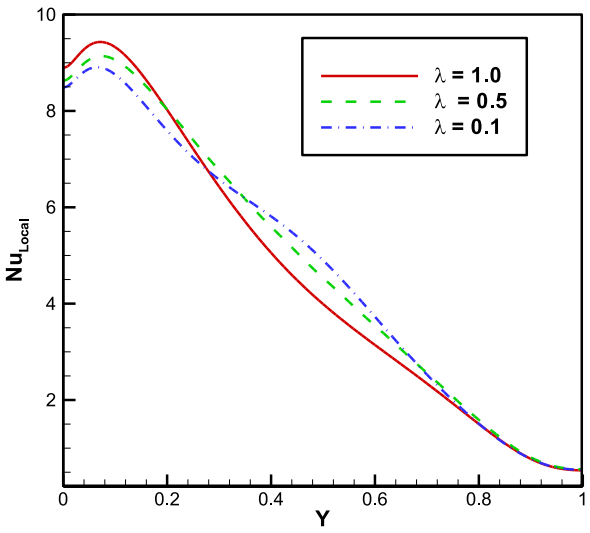

Fig. 10. The local Nusselt number (Nu_{Local}) along the hot wall.

11. Two correlations for Nu_{ave} and N_{gen} were proposed that their R^2 values are 0.9814 and 0.9789, respectively [Eqs. (31) and (32)].

CRediT authorship contribution statement

Seyyed Masoud Seyyedi: Writing – original draft, Visualization, Validation, Software, Formal analysis, Investigation. **Mehdi Hashemi-Tilehnoee:** Writing – original draft, Validation, Software, Investigation. **Elena Palomo del Barrio:** Writing – review & editing, Supervision, Methodology. **Humaira Yasmin:** Writing – review & editing, Funding acquisition, Investigation. **Mohsen Sharifpur:** Writing – review & editing, Supervision, Conceptualization.

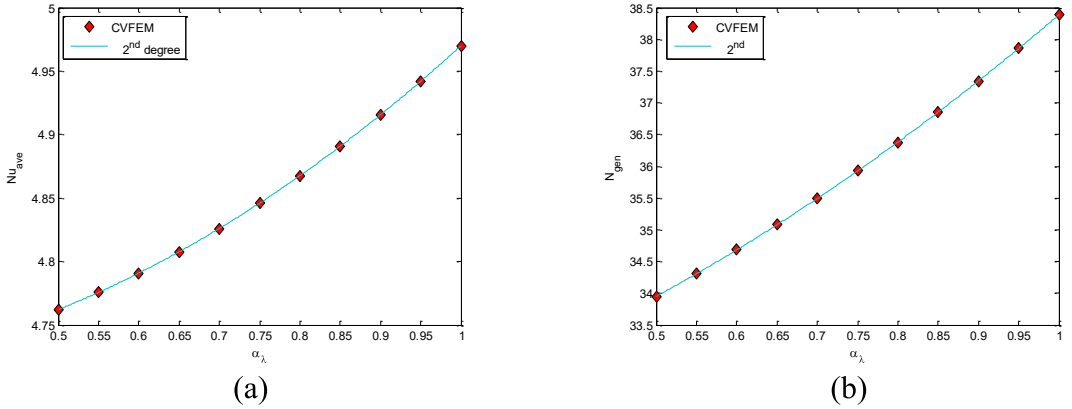

Fig. 11. The variations of Nu_{ave} and N_{gen} versus α_λ

Table 8
Correlations for Nu_{ave} and N_{gen}

$\alpha_\lambda = \frac{\phi_1}{\phi_1+\phi_2}$ where $0.5 < \alpha_\lambda < 1$, $\phi_1 + \phi_2 = 0.04$, $\phi_3 = 0.01$	a_2	a_1	a_0
$Nu_{ave} = a_2\alpha_\lambda^2 + a_1\alpha_\lambda + a_0$	0.32065	−0.065234	4.7146
$N_{gen} = a_2\alpha_\lambda^2 + a_1\alpha_\lambda + a_0$	3.8615	3.0828	31.444

Declaration of competing interest

The authors declare that they have no known competing financial interests or personal relationships that could have appeared to influence the work reported in this paper.

Acknowledgment

The authors acknowledge support from the Deanship of Scientific Research, the Vice Presidency for Graduate Studies and Scientific Research, King Faisal University, Saudi Arabia (Grant No. KFU250783).

Data availability

Data will be made available on request.

References

[1] M. Izadi, A. Behzadmehr, D. Jalali-Vahida, Numerical study of developing laminar forced convection of a nanofluid in an annulus, Int. J. Therm. Sci. 48 (11) (2009) 2119–2129.
[2] R. Nasrin, M.A. Alim, A.J. Chamkha, Numerical simulation of non-Darcy forced convection through a channel with non-uniform heat flux in an open cavity using nanofluid, Numer Heat Transf. Part A Appl. 64 (2013) 820–840.
[3] M. Sheikholeslami, A.J. Chamkha, Influence of Lorentz forces on nanofluid forced convection considering Marangoni convection, J. Mol. Liq. 225 (2017) 750–757.
[4] R. Mohebbi, et al., Forced convection of nanofluids in an extended surfaces channel using lattice Boltzmann method, Int. J. Heat Mass Tran. 117 (2018) 1291–1303.
[5] N.S. Shashikumar, B.J. Gireesha, B. Mahanthesh, B.C. Prasannakumara, J. Chamkha Ali, Entropy generation analysis of magneto-nanoliquids embedded with aluminium and titanium alloy nanoparticles in microchannel with partial slips and convective conditions, Int. J. Numer. Methods Heat Fluid Flow 29 (2019) 3638–3658, https://doi.org/10.1108/HFF-06-2018-0301.
[6] Benhanifia Kada, Fares Redouane, Lakhdar Rahmani, Naveen Kumar Gupta, Mebarki Brahim, Hitesh Panchal, Saeed Nazari, Abhinav Kumar, Anand Patel, Numerical investigation of forced convection flow of a complex Bingham–Papanastasiou fluid between two concentric cylinders with a wavy inner wall, J. Therm. Eng. 10 (1) (January, 2024) 142–152.
[7] G. de Vahl Davis, Natural convection in a square cavity: a benchmark solution, Int. J. Numer. Methods Fluid. 3 (3) (1983) 249–264, https://doi.org/10.1002/fld.1650030305.
[8] B.S. Yilbas, S.Z. Shuja, S.A. Gbadebo, H.I.A. Al-Hamayle, K. Boran, Natural convection and entropy generation in a square cavity, Int. J. Energy Res. 22 (1998) 1275–1290 [CrossRef].
[9] O. Aydin, I. Pop, Natural convection in a differentially heated enclosure filled with a micropolar fluid, Int. J. Therm. Sci. 46 (10) (2007) 963–969, https://doi.org/10.1016/j.ijthermalsci.2006.11.018.
[10] Mohsen Pirmohammadi, Majid Ghassemi, Ghanar A. Sheikhzadeh, The effect of a magnetic field on buoyancy-driven convection in differentially heated square cavity. Electromagnetic Launch Technology, 2008 14th Symposium on, IEEE, 2008, pp. 1–6.
[11] G.G. Ilis, Effect of aspect ratio on entropy generation in a rectangular cavity with differentially heated vertical walls, Int. Commun. Heat Mass Tran. 35 (2008) 696–703.

[12] B. Ghasemi, S.M. Aminossadati, Natural convection heat transfer in an inclined enclosure filled with a water–CuO nanofluid, Numer Heat Transf Part A Appl. 55 (2009) 807–823.
[13] R. Nasrin, S. Parvin, Investigation of buoyancy-driven flow and heat transfer in a trapezoidal cavity filled with water–Cu nanofluid, Int. Commun. Heat Mass Tran. 39 (2012) 270–274.
[14] S. Jani, M. Mahmoodi, M. Amini, M. Akbari, Free convection in rectangular enclosures containing nanofluid with nanoparticles of various diameters, Heat Tran. Res. 45 (2) (2014).
[15] A. Chamkha, M. Ismael, A. Kasaeipoor, T. Armaghani, Entropy generation and natural convection of CuO-water nanofluid in C-shaped cavity under magnetic field, Entropy 18 (2016) 50–67.
[16] M.S. Astanina, M.A. Sheremet, H.F. Oztop, N. Abu-Hamdeh, MHD natural convection and entropy generation of ferrofluid in an open trapezoidal cavity partially filled with a porous medium, Int. J. Mech. Sci. 136 (2018) 493–502.
[17] A.S. Dogonchi, M.A. Sheremet, I. Pop, D.D. Ganji, MHD natural convection of Cu/H2O nanofluid in a horizontal semi-cylinder with a local triangular heater, Int. J. Numer. Methods Heat Fluid Flow 28 (2018) 2979–2996, https://doi.org/10.1108/HFF-04-2018-0160.
[18] F. Selimefendigil, H.F. Oztop, A.J. Chamkha, Natural convection in a CuO–water nanofluid filled cavity under the effect of an inclined magnetic field and phase change material (PCM) attached to its vertical wall, J. Cermal Anal. Calorimetr. 135 (2) (2019).
[19] S.M. Seyyedi, A.S. Dogonchi, D.D. Ganji, M. Hashemi-Tilehnoee, Entropy generation in a nanofluid-filled semi-annulus cavity by considering the shape of nanoparticles, J. Therm. Anal. Calorim. 138 (2019) 1607–1621.
[20] Seyyed Masoud Seyyedi, A.S. Dogonchi, R. Nuraei, D.D. Ganji, M. Hashemi-Tilehnoee, Numerical analysis of entropy generation of a nanofluid in a semi-annulus porous enclosure with different nanoparticle shapes in the presence of a magnetic field, Eur. Phys. J. Plus 134 (2019) 268.
[21] M. Hashemi-Tilehnoee, S. Tashakor, A.S. Dogonchi, Seyyed Masoud Seyyedi, M. Khaleghi, Entropy generation in concentric annuli of 400 kV gas-insulated transmission line, Therm. Sci. Eng. Prog. 19 (2020) 100614.
[22] A.S. Dogonchi, M. Hashemi-Tilehnoee, M. Waqas, S.M. Seyyedi, I.L. Animasaun, D.D. Ganji, The influence of different shapes of nanoparticle on Cu–H2O nanofluids in a partially heated irregular wavy enclosure, Physica A 540 (2020) 123034.
[23] M. Mahmoodi, Numerical simulation of free convection of a nanofluid in L-shaped cavities, Int. J. Therm. Sci. 50 (2011) 1731–1740, https://doi.org/10.1016/jijthermalsci.2011.04.009.
[24] M. Ahmed, M. Eslamian, Natural convection in a differentially heated square enclosure filled with a nanofluid: significance of the thermophoresis force and slip/drift velocity, Int. Commun. Heat Mass Tran. 58 (2014) 1–11, https://doi.org/10.1016/j.icheatmasstransfer.2014.08.008.
[25] I.D. Garbadeen, M. Sharifpur, J.M. Slabber, J.P. Meyer, Experimental study on natural convection of MWCNT-water nanofluids in a square enclosure, Int. Commun. Heat Mass Tran. 88 (2017) 1–8, https://doi.org/10.1016/j.icheatmasstransfer.2017.07.019.
[26] I.M. Safwan, I.A. Alsabery, A. Chamkha, H. Ishak, Effect of finite wall thickness on entropy generation and natural convection in a nanofluid-filled partially heated square cavity, Int. J. Numer. Methods Heat Fluid Flow 30 (2019) 1518–1546, https://doi.org/10.1108/HFF-06-2019-0505.
[27] M. Hashemi-Tilehnoee, A. Dogonchi, S.M. Seyyedi, A.J. Chamkha, D. Ganji, Magnetohydrodynamic natural convection and entropy generation analyses inside a nanofluid-filled incinerator-shaped porous cavity with wavy heater block, J. Therm. Anal. Calorim. 141 (5) (2020) 2033–2045.
[28] M. Sheikholeslami, S.A. Shehzad, Non-Darcy free convection of Fe3O4-water nanoliquid in a complex shaped enclosure under impact of uniform Lorentz force, Chin. J. Phys. 56 (2018) 270–281.
[29] S.M. Seyyedi, On the entropy generation for a porous enclosure subject to a magnetic field: different orientations of cardioid geometry, Int. Commun. Heat Mass Tran. 116 (2020). Article ID 104712.
[30] H. Goodarzi, O.A. Akbari, M.M. Sarafraz, M.M. Karchegani, M.R. Safaei, G.A. Sheikh Shabani, Numerical simulation of natural convection heat transfer of nanofluid with Cu, MWCNT, and Al2O3nanoparticles in a cavity with different aspect ratios, J. Therm. Sci. Eng. Appl. 11 (6) (2019).
[31] S.M. Seyyedi, A.S. Dogonchi, M. Hashemi-Tilehnoee, M. Waqas, D.D. Ganji, Entropy generation and economic analyses in a nanofluid filled L-shaped enclosure subjected to an oriented magnetic field, Appl. Therm. Eng. 168 (2020) 114789.
[32] Chikr Djaoutsi Zineb, Fares Redouane, Hidki Rachid, Naim Houcine, Exploring the complex interplay of factors in convective heat transfer: a comprehensive parametric analysis in three-dimensional permeable cavities, Energy Sources, Part A Recovery, Util. Environ. Eff. 46 (1) (2024) 6064–6080, https://doi.org/10.1080/15567036.2024.2346181.
[33] K.M. Khanafer, A.J. Chamkha, Mixed convection flow in a lid-driven enclosure filled with a fluid-saturated porous medium, Int. J. Heat Mass Tran. 42 (13) (1999) 2465–2481.
[34] N.S. Gibanov, M.A. Sheremet, H.F. Oztop, N. Abu-Hamdeh, Effect of uniform inclined magnetic field on mixed convection in a lid-driven cavity having a horizontal porous layer saturated with a ferrofluid, Int. J. Heat Mass Tran. 114 (2017) 1086–1097.
[35] S. Nazari, R. Ellahi, M. Sarafraz, M.R. Safaei, A. Asgari, O.A. Akbari, Numerical study on mixed convection of a non-Newtonian nanofluid with porous media in a two lid-driven square cavity, J. Therm. Anal. Calorim. (2019) 1–25.
[36] M.H. Esfe, A.H. Refahi, H. Teimouri, M. Javad Noroozi, M. Afrand, A. Karimipour, Mixed convection fluid flow and heat transfer of the Al2O3-water nanofluid with variable properties in a cavity with an inside quadrilateral obstacle, Heat Tran. Res. 46 (5) (2015).
[37] F. Selimefendigil, H.F. Öztop, A.J. Chamkha, MHD mixed convection and entropy generation of nanofluid filled lid driven cavity under the influence of inclined magnetic fields imposed to its upper and lower diagonal triangular domains, J. Magn. Magn Mater. 406 (2016) 266–281, https://doi.org/10.1016/j.jmmm.2016.01.039.
[38] M.A. Ismael, E. Abu-nada, A.J. Chamkha, Mixed convection in a square cavity filled with CuO-water nanofluid heated by corner heater, Int. J. Mech. Sci. 133 (2017) 42–50, https://doi.org/10.1016/j.ijmecsci2017.08.029.
[39] M. Izadi, A. Behzadmehr, M.M. Shahmardan, Effects of discrete source-sink arrangements on mixed convection in a square cavity filled by nanofluid, Kor. J. Chem. Eng. 31 (1) (2014) 12–19.
[40] S. Hussain, K. Mehmood, M. Sagheer, MHD mixed convection and entropy generation of water–alumina nanofluid flow in a double lid driven cavity with discrete heating, J. Magn. Magn Mater. 419 (2016) 140–155.
[41] M. Hashemi-Tilehnoee, E.P. del Barrio, Magneto laminar mixed convection and entropy generation analyses of an impinging slot jet of Al_2O_3-water and Novec-649, Therm. Sci. Eng. Prog. 36 (2022) 101524.
[42] M. Hashemi-Tilehnoee, S.M. Seyyedi, E. Palomo Del Barrio, F. Hosseinnejad, M. Sharifpur, Electro-magnetic enhanced mixed-convection of a confined slot NEPCM-water impinging jet equipped with metal foam, J. Appl. Comput. Mech. (2024), https://doi.org/10.22055/jacm.2024.46885.4616.
[43] M. Zadravec, M. Hribersek, L. Skerget, Natural convection of micropolar fluid in an enclosure with boundary element method, Eng. Anal. Bound. Elem. 33 (2009) 485–492.
[44] S.M. Shavik, M. Nasim Hassan, A.K.M. Monjur Morshed, M. Quamrul Islam, Natural convection and entropy generation in a square inclined cavity with differentially heated vertical walls, Procedia Eng. 90 (2014) 557–562.
[45] S.U.S. Choi, Enhancing thermal conductivity of fluids with nanoparticles, ASME Fluids Eng. Div. 231 (1995) 99–103.
[46] K.Y. Leong, R. Saidur, S.N. Kazi, A.H. Mamun, Performance investigation of an automotive car radiator operated with nanofluid-based coolants (nanofluid as a coolant in a radiator), Appl. Therm. Eng. 30 (2010) 2685–2692.
[47] R. Saidur, K.Y. Leong, H.A. Mohammad, A review on applications and challenges of nanofluids, Renew. Sustain. Energy Rev. 15 (2011) 1646–1668.
[48] T. Yousefi, F. Veysi, E. Shojaeizadeh, S. Zinadini, An experimental investigation on the effect of Al_2O_3-H2O nanofluid on the efficiency of flat-plate solar collectors, Renew. Energy 39 (2012) 293–298.
[49] K. Torrance, R. Davis, K. Eike, P. Gill, D. Gutman, A. Hsui, et al., Cavity flows driven by buoyancy and shear, J. Fluid Mech. 51 (2) (1972) 221–231.
[50] K. Khanafer, K. Vafai, M. Lightstone, Buoyancy-driven heat transfer enhancement in a two-dimensional enclosure utilizing nanofluids, Int. J. Heat Mass Tran. 46 (2003) 3639–3653, https://doi.org/10.1016/S0017-9310(03)00156-X.
[51] Fares Redouane, Chikr Djaoutsi Zineb, Hidki Rachid, Vehicle engine cooling system: review research, J. Nanof. 13 (2024) 625–637.

[52] Iskander Tlili, Seyyed Masoud Seyyedi, A.S. Dogonchi, M. Hashemi-Tilehnoee, D.D. Ganji, Analysis of a single-phase natural circulation loop with hybrid-nanofluid, Int. Commun. Heat Mass Tran. 112 (2020) 104498.

[53] R.S.R. Gorla, S. Siddiq, M.A. Mansour, A.M. Rashad, T. Salah, Heat source/sink effects on a hybrid nanofluid-filled porous cavity, J. Thermophys. Heat Tran. 31 (4) (2017) 847–857.

[54] S.A.M. Mehryan, F.M. Kashkooli, M. Ghalambaz, A.J. Chamkha, Free convection of hybrid Al2O3-Cu water nanofluid in a differentially heated porous cavity, Adv. Powder Technol. 28 (2017) 2295–2305.

[55] T. Tayebi, A.J. Chamkha, Free convection enhancement in an annulus between horizontal confocal elliptical cylinders using hybrid nanofluids, Numer. Heat Tran. 70 (2016) 1141–1156.

[56] T. Tayebi, A.J. Chamkha, Natural convection enhancement in an eccentric horizontal cylindrical annulus using hybrid nanofluids, Numer. Heat Tran. 71 (11) (2017) 1159–1173.

[57] A.J. Chamkha, A.S. Dogonchi, D.D. Ganji, Magneto-hydrodynamic flow and heat transfer of a hybrid nanofluid in a rotating system among two surfaces in the presence of thermal radiation and Joule heating, AIP Adv. 9 (2) (2019) 025103.

[58] Fares Redouane, Hidki Rachid, Aissani Abdelkader, Numerical simulation of combined convection and radiation heat transfer in a hybrid nanofluid inside an open fins cavity under a magnetic field, J. Therm. Anal. Calorim. 149 (2024) 8523–8538, https://doi.org/10.1007/s10973-024-13158-9.

[59] Hui Chen, Panfeng He, Ming Shen, Yiren Ma, Thermal analysis and entropy generation of Darcy-Forchheimer ternary nanofluid flow: a comparative study, Case Stud. Therm. Eng. 43 (2023) 102795.

[60] M.M. Souby, M. Bargal, Y.P. Wang, Thermohydraulic performance improvement and entropy generation characteristics of a microchannel heat sink cooled with new hybrid nanofluids containing ternary/binary hybrid nanocomposites, Energy Sci. Eng. 9 (12) (2021) 2493–2513.

[61] W. Ashraf Adnan, Thermal efficiency in hybrid (Al2O3-CuO/H2O) and ternary hybrid nanofluids (Al2O3-CuO-Cu/H2O) by considering the novel effects of imposed magnetic field and convective heat condition, Wave Random Complex (2022) 1–16.

[62] T. Elnaqeeb, I.L. Animasaun, N.A. Shah, Ternary-hybrid nanofluids: significance of suction and dual-stretching on three-dimensional flow of water conveying nanoparticles with various shapes and densities, Z. Naturforsch. 76 (3) (2021) 231–243.

[63] S.A.M. Mehryan, M. Izadi, A.J. Chamkha, M.A. Sheremet, Natural convection and entropy generation of a ferrofluid in a square enclosure under the effect of a horizontal periodic magnetic field, J. Mol. Liq. 263 (2018) 510–525.

[64] Seyyed Masoud Seyyedi, Mehdi Hashemi Tilehnoee, Investigating the effect of magnetic field on the natural convection and entropy generation in a Al2O3–Water nanofluid enclosure, Appl. Energy Conversion 1 (2023) 6253.1019.

[65] B. Kim, D. Lee, M. Ha, H. Yoon, A numerical study of natural convection in a square enclosure with a circular cylinder at different vertical locations, Int. J. Heat Mass Tran. 5 (2008) 1888–1906.

[66] S. Soleimani, M. Sheikholeslami, D.D. Ganji, M. Gorji-Bandpay, Natural convection heat transfer in a nanofluid filled semi-annulus enclosure, Int. Commun. Heat Mass Tran. 39 (2012) 565–574.

[67] Mohsen Pirmohammadi, Majid Ghassemi, Effect of magnetic field on convection heat transfer inside a tilted square enclosure, Int. Commun. Heat Mass Tran. 36 (2009) 776–780.

[68] A.S. Dogonchi, T. Armaghani, A.J. Chamkha, D.D. Ganji, Natural convection analysis in a cavity with an inclined elliptical heater subject to shape factor of nanoparticles and magnetic field, Arabian J. Sci. Eng. (2019), https://doi.org/10.1007/s13369-019-03956-x.

[69] A.S. Dogonchi, T. Tayebi, A.J. Chamkha, D.D. Ganji, Natural convection analysis in a square enclosure with a wavy circular heater under magnetic field and nanoparticles, J. Therm. Anal. Calorim. (2019), https://doi.org/10.1007/s10973-01908408-0.

[70] T.-H. Hsu, C.-K. Chen, Natural convection of micropolar fluids in a rectangular enclosure, Int. J. Eng. Sci. 34 (1996) 407–415.

[71] A.C. Baytas, I. Pop, Free convection in a square porous cavity using a thermal nonequilibrium model, Int. J. Therm. Sci. 41 (2002) 861–870.

[72] S.H. Tasnim, S. Mahmud, Laminar free convection inside an inclined L-shaped enclosure, Int. Commun. Heat Mass Tran. 33 (2006) 936–942.

[73] S. Mahmud, S.H. Tasnim, Free convection in a cavity with two straight and two arced walls, Int. Commun. Heat Mass Tran. 31 (2004) 525–536.

[74] P. Ternik, Conduction and convection heat transfer characteristics of water–Au nanofluid in a cubic enclosure with differentially heated side walls, Int. J. Heat Mass Tran. 80 (2015) 368–375, https://doi.org/10.1016/j.ijheatmasstransfer.2014.09.041.

[75] K. Ghasemi, M. Siavashi, Lattice Boltzmann numerical simulation and entropy generation analysis of natural convection of nanofluid in a porous cavity with different linear temperature distributions on side walls, J. Mol. Liq. (2017), https://doi.org/10.1016/j.molliq.2017.03.016.

[76] M. Mahmoodi, S.M. Hashemi, Numerical study of natural convection of a nanofluid in C-shaped enclosures, Int. J. Therm. Sci. 55 (2012) 76–89, https://doi.org/10.1016/j.ijthermalsci.2012.01.002.

[77] R. Mohebbi, M.M. Rashidi, Numerical simulation of natural convection heat transfer of a nanofluid in an L-shaped enclosure with a heating obstacle, J. Taiwan Inst. Chem. Eng. 72 (2017) 70–84, https://doi.org/10.1016/j.jtice.2017.01.006.

[78] M. Sheikholeslami, Z. Li, M. Shamlooei, Nanofluid MHD natural convection through a porous complex shaped cavity considering thermal radiation, Phys. Lett. A 382 (2018) 1615–1632.

[79] A.M. Rashad, T. Armaghani, A.J. Chamkha, M.A. Mansour, Entropy generation and MHD natural convection of a nanofluid in an inclined square porous cavity: effects of a heat sink and source size and location, Chin. J. Phys. 56 (2018) 193–211, https://doi.org/10.1016/jcjph.2017.11.026.

[80] M.A. Sheremet, M.S. Astanina, I. Pop, MHD natural convection in a square porous cavity filled with a water-based magnetic fluid in the presence of geothermal viscosity, Int. J. Numer. Methods Heat Fluid Flow 28 (2018) 2111–2131, https://doi.org/10.1108/HFF-12-2017-0503.

[81] S.A.M. Mehryan, M. Izadi, Z. Namazian, A.J. Chamkha, Natural convection of multi-walled carbon nanotube–Fe3O4/water magnetic hybrid nanofluid flowing in porous medium considering the impacts of magnetic field-dependent viscosity, J. Therm. Anal. Calorim. 138 (2019) 1541–1555, https://doi.org/10.1007/s10973-019-08164-1.

[82] M. Ghalambaz, S.A.M. Mehryan, E. Izadpanahi, A.J. Chamkha, D. Wen, MHD natural convection of Cu–Al2O3 water hybrid nanofluids in a cavity equally divided into two parts by a vertical flexible partition membrane, J. Therm. Anal. Calorim. (2019), https://doi.org/10.1007/s10973-019-08258-w.

[83] M. Izadi, R. Mohebbi, A.A. Delouei, H. Sajjadi, Natural convection of a magnetizable hybrid nanofluid inside a porous enclosure subjected to two variable magnetic fields, Int. J. Mech. Sci. 151 (2019) 154–169.

[84] M. Sheikholeslami, S.A. Mehryan, A. Shafee, M.A. Sheremet, Variable magnetic forces impact on magnetizable hybrid nanofluid heat transfer through a circular cavity, J. Mol. Liq. 277 (2019) 388–396.

[85] M. Izadi, N.M. Maleki, I. Pop, S.A. Mehryan, Natural convection of a hybrid nanofluid subjected to non-uniform magnetic field within porous medium including circular heater, Int. J. Numer. Methods Heat Fluid Flow 29 (2019) 1211–1231.

[86] H. Sajjadi, A.A. Delouei, M. Izadi, R. Mohebbi, Investigation of MHD natural convection in a porous media by double MRT lattice Boltzmann method utilizing MWCNT–Fe3O4/water hybrid nanofluid, Int. J. Heat Mass Tran. 132 (2019) 1087–1104.

[87] M. Izadi, S. Mehryan, M.A. Sheremet, Natural convection of CuO-water micropolar nanofluids inside a porous enclosure using local thermal non-equilibrium condition, J. Taiwan Inst. Chem. Eng. 88 (2018) 89–103.

[88] M. Izadi, M.A. Sheremet, S. Mehryan, I. Pop, H.F. Öztop, N. Abu-Hamdeh, MHD thermos gravitational convection and thermal radiation of a micropolar nanoliquid in a porous chamber, Int. Commun. Heat Mass Tran. 110 (2020) 104409.

[89] S.M. Seyyedi, M. Hashemi-Tilehnoee, E. Palomo del Barrio, A.S. Dogonchi, M. Sharifpur, Analysis of magneto-natural-convection flow in a semi-annulus enclosure filled with a micropolar-nanofluid; a computational framework using CVFEM and FVM, J. Magn. Magn Mater. 568 (2023), https://doi.org/10.1016/j.jmmm2023.170407.

[90] Mehdi Hashemi-Tilehnoee, Seyyed Masoud Seyyedi, Elena Palomo del Barrio, Mohsen Sharifpur, Analysis of natural convection and the generation of entropy within an enclosure filled with nanofluid-packed structured pebble beds subjected to an external magnetic field and thermal radiation, J. Energy Storage 73 (2023) 109223.

[91] Mohsen Izadi, Mikhail A. Sheremet, S.A.M. Mehryan, Natural convection of a hybrid nanofluid affected by an inclined periodic magnetic field within a porous medium, Chin. J. Phys. 65 (2020) 447–458.

[92] M. Ghalambaz, A.J. Chamkha, D. Wen, Natural convective flow and heat transfer of nano-encapsulated phase change materials (NEPCMs) in a cavity, Int. J. Heat Mass Tran. 138 (2019) 738–749, https://doi.org/10.1016/j.ijheatmasstransfer.2019.04.037.
[93] A. Doostani, M. Ghalambaz, A.J. Chamkha, MHD natural convection phase - change heat transfer in a cavity: analysis of the magnetic field effect, J. Brazilian Soc. Mech. Sci. Eng. (2017), https://doi.org/10.1007/s40430-017-0722-z.
[94] A.J. Chamkha, A. Doostani dezfuli, E. Izadpanahi, M. Ghalambaz, Phase-change heat transfer of single/hybrid nanoparticles enhanced phase-change materials over a heated horizontal cylinder confined in a square cavity, Adv. Powder Technol. 28 (2017) 385–397, https://doi.org/10.1016/j.apt.2016.10.009.
[95] M. Ghalambaz, A. Doostani, A.J. Chamkha, M.A. Ismael, Melting of nanoparticles-enhanced phase-change materials in an enclosure: effect of hybrid nanoparticles, Int. J. Mech. Sci. 134 (2017) 85–97.
[96] S.M. Seyyedi, M. Hashemi-Tilehnoee, M. Sharifpur, Impact of fusion temperature on hydrothermal features of flow within an annulus loaded with nanoencapsulated phase change materials (NEPCMs) during natural convection process, Math. Probl Eng. 2021 (2021), https://doi.org/10.1155/2021/4276894.
[97] M. Hashemi-Tilehnoee, S.M. Seyyedi, E. Palomo del Barrio, M. Sharifpur, Heat transfer intensification of NEPCM-water suspension filled heat sink cavity with notches cooling tubes by applying the electric field, J. Energy Storage 59 (2023), https://doi.org/10.1016/j.est.2022.106492.
[98] M. Ghalambaz, A. Doostanidezfuli, H. Zargartalebi, A.J. Chamkha, MHD phase change heat transfer in an inclined enclosure: effect of a magnetic field and cavity inclination, Numer Heat Transf. Part A Appl. 71 (2017) 91–109, https://doi.org/10.1080/104077822016.1244397.
[99] M. Hashemi-Tilehnoee, A.S. Dogonchi, S.M. Seyyedi, M. Sharifpur, Magneto-fluid dynamic and second law analysis in a hot porous cavity filled by nanofluid and nano-encapsulated phase change material suspension with different layout of cooling channels, J. Energy Storage 31 (2020), https://doi.org/10.1016/jest2020.101720.
[100] S.M. Seyyedi, M. Hashemi-Tilehnoee, M. Sharifpur, Effect of inclined magnetic field on the entropy generation in an annulus filled with NEPCM suspension, Math. Probl Eng. 2021 (2021), https://doi.org/10.1155/2021/8103300.
[101] K.T. Yang, Natural convection in enclosures, in: S. Kakaç, R. Shah, W. Aung (Eds.), Handbook of Single-phase Convective Heat Transfer, John Wiley, New York, 1987 (Chapter 13).
[102] S. Ostrach, Natural convection in enclosures, J. Heat Tran. 110 (1988) 1175–1190.
[103] T. Fusegi, J.M. Hyun, Laminar and transitional natural convection in an enclosure with complex and realistic conditions, Int. J. Heat Fluid Flow 15 (1994) 258–268.
[104] D. Das, M. Roy, T. Basak, Studies on natural convection within enclosures of various (non-square) shapes - a review, Int. J. Heat Mass Tran. 106 (2016) 356–406, https://doi.org/10.1016/jijheatmasstransfer.2016.08.034.
[105] S. O. Giwa, M. Sharifpur, M. H. Ahmadi, J. P. Meyer, A review of magnetic field influence on natural convection heat transfer performance of nanofluids in square cavities, J. Therm. Anal. Calorim., https://doi.org/10.1007/s10973-020-09832-3.
[106] Guannan Wang, Zhen Zhang, Ruijin Wang, Zefei Zhu, A review on heat transfer of nanofluids by applied electric field or magnetic field, Nanomaterials 10 (2020) 2386.
[107] H.J. Saabas, B.R. Baliga, Co-located equal-order control-volume finite-element method for multidimensional, incompressible. Fluid flow-part i: formulation, Numer, Heat Transfer 26 (4) (1994) 381–407.
[108] M.S. Kandelousi, Effect of spatially variable magnetic field on ferrofluid flow and heat transfer considering constant heat flux boundary condition, Eur. Phys. J. Plus 129 (11) (2014) 1–12.